Aerosol Science 40 (2009) 664 – 679

Contents lists available at ScienceDirect

Aerosol Science

journal homepage: www.elsevier.com/locate/jaerosci

Parameterization of aerosol dry deposition velocities onto smooth and rough surfaces

V.N. Piskunov

Russian Federal Nuclear Center - VNIIEF, 37 Mir Ave., Sarov 607190, Nizhni Novgorod region, Russia

ARTICLE INFO

Article history:
Received 12 December 2008
Received in revised form
8 April 2009
Accepted 9 April 2009

Keywords:
Aerosol
Diffusion
Turbophoresis
Dry deposition
Surface roughness
Urban environment

ABSTRACT

The velocities of aerosol deposition onto vertical and horizontal surfaces are needed for 2D and 3D calculations of aerosol transport and deposition in the urban and indoor environments. This paper analyzes the experimental results and semiempirical and theoretical models on dry deposition velocities. The features of the solution obtained by Zhao and Wu [(2006a). Modeling particle deposition from fully developed turbulent flow in ventilation duct. *Atmospheric Environment, 40*, 457–466] for the velocity of aerosol deposition onto smooth surfaces are analyzed, the integrals are approximated analytically. To treat the deposition onto rough surfaces, the results of Sehmel [(1973). Particle eddy diffusivities and deposition for isothermal flow and smooth surfaces. *Journal of Aerosol Science*, *4*, 125–138]; Sehmel and Hodgson [(1978). A model for predicting dry deposition of particles and gases to environmental surfaces. PNL-SA-6721. Richland, WA: Battelle, Pacific Northwest Laboratory] are modified and represented in a unified manner for vertical and horizontal surfaces. Cross-comparison with data of Slinn [(1978) Parameterization for resuspension and for Wet and Dry Deposition of Particles and Gases for Use in Radiation Dose Calculations. *Nucl.Safety*, 19(2), 205–219.] and the model of Lai and Nazaroff [(2000). Modeling indoor particle deposition from turbulent flow onto smooth surfaces. *Journal of Aerosol Science*, *31*, 463–476] allowed reconciliation between the theoretical and semiempirical approaches. Finally, an approximation to the aerosol dry deposition velocities is obtained in the form of convenient parameterization formulas covering a wide range of particle sizes $0.01\,\mu\text{m} \leqslant d \leqslant 1000\,\mu\text{m}$ and surface roughnesses $z_0 \leqslant 10$ cm.

1. Introduction

The calculation of aerosol deposition in the urban environment (Jonsson, Karlsson, & Jönsson, 2008; Kosovic et al., 2005; Yang & Shao, 2008) and indoors (Chen, Yu & Lai, 2006; Gao & Niu, 2007; Zhao & Wu, 2007) requires expressions for the dry deposition velocity which must satisfy rather diverse requirements:

- possibility of calculating the deposition onto vertical walls and horizontal surfaces;
- possibility of calculating different degrees of surface roughness z_0 ranging from 0 to 1 m and arbitrary particle size d ranging from 10^{-8} to 10^{-3} m;
- simple formulas allowing real-time computations.

E-mail address: piskunov@vniief.ru

0021-8502/$ - see front matter
doi:10.1016/j.jaerosci.2009.04.006

Nomenclature

C	aerosol concentration
C_c	Cunningham correction coefficient: $C_c = 1 + 2\frac{\lambda}{d}\left[1.257 + 0.4\exp\left(-\frac{1.1d}{2\lambda}\right)\right]$
C_D	particle drag coefficient: $C_D(Re) = 24/Re + C^0$, where $C^0 = 0.42$
d	particle diameter
D	coefficient of Brownian diffusion of aerosol particles: $D = kTC_c/3\pi\mu d$
g	gravitational acceleration
g^+	dimensionless gravitational acceleration $g^+ = g\nu/(u^*)^3$
k	Boltzmann constant
j	aerosol particle flux
k^+	dimensionless roughness parameter $k^+ = z_0 u^*/\nu$
L	Monin–Obukhov parameter
Re	Reynolds number $Re = d\rho u_s/\mu$ for particle deposition
Sc	Schmidt number $Sc = \nu/D$
T	ambient temperature
u^*	friction velocity in the surface (near-wall) layer
u_d, α	pollutant dry deposition velocity
u_d^+	pollutant dry deposition velocity in dimensionless units, $u_d^+ = u_d/u^*$
u_s	particle gravity sedimentation velocity $u_s = \frac{12\mu}{C^0 C_c \rho d}\left(\sqrt{1 + \frac{C^0 C_c^2 \rho\rho_p}{108\mu^2} d^3\left(1 - \frac{\rho}{\rho_p}\right) g} - 1\right)$
y	distance to the surface (wall)
y^+	dimensionless distance to the surface (wall) $y^+ = yu^*/\nu$
z_0	surface roughness parameter
α, u_d	pollutant dry deposition velocity
λ	air molecular path
μ	air dynamic viscosity
ν	air kinematic (molecular) viscosity $\nu = \mu/\rho$
ν_t	air turbulent viscosity
ρ	air density
ρ_p	particle density
τ_p	characteristic time of particle relaxation (deceleration) $\tau_p = u_s/g$
τ_L	Lagrangian timescale of turbulence
τ^+	dimensionless relaxation time $\tau^+ = \tau_p u^{*2}/\nu$

Numerous papers (Davies, 1966; Fan & Ahmadi, 1993; Johansen, 1991; Kharchenko, 1997; Liu & Agarwal, 1974; Nho-Kim, Michou, and Peuch, 2004; Sehmel, 1973, 1980; Sehmel & Hodgson, 1978; Sippola & Nazaroff, 2002; Slinn, 1978, 1982; Valentine and Smith, 2005; Wood, 1981a, 1981b; Zaichik and Alipchenkov, 2007) describe semiempirical relations for the velocities of deposition onto vertical and horizontal walls. These were determined mainly from experimental data on turbulent deposition in ducts and channels. The most complete set of data was obtained by Sehmel (1973) and by Sehmel and Hodgson (1978), including those from open-surface experiments. Note that in the various semiempirical formulas it is not always possible to determine their range of validity or take into account the complete set of the physical effects within the turbulent boundary layer.

Most attractive are the theoretical models considering the physical pattern of the particle motion and deposition in the near-wall layer formed near a surface. With these models it becomes possible to include particle motion in a heterogeneous turbulence field (turbophoresis), including the particle lag in turbulent pulsations. One of the most complete models of this kind is the generalized Eulerian theory presented by Guha (1997). However, this theory is difficult to close and use within the numerical complexes computing the 2D and 3D pattern of turbulent flows in the urban environment. It would be most helpful to have a self-contained technique for computing the deposition velocity with a minimum of input parameters.

An important step in this direction is the paper by Lai and Nazaroff (2000), who consider the particle deposition onto horizontal and vertical surfaces of rooms, when turbophoresis can be neglected. Since its application requires a detailed description only of the respirable aerosol fraction dangerous in inhalation, this model can serve as a simple, easy-to-use tool.

A very important contribution to the development of easy-to-use deposition models which at the same time include the entire set of factors important in practice has been made by Zhao and Wu (2006a, 2006b). Zhao and Wu (2006a) suggest an improved Eulerian model to predict the particle deposition velocity onto walls in a developed turbulent flow. The model partitions the boundary layer into three areas and includes the description of turbophoresis, Brownian and turbulent diffusion as well as sedimentation. A relation between the turbophoresis velocity to the deceleration time, friction velocity and normal distance to the surface is used. The predicted results agree well with the measured data for the internal surfaces of buildings and for vertical walls of channels. The model is easy to use and operates with a combination of dimensionless quantities. The only input parameters required are the friction velocity, particles diameter and density. The model was further improved by Zhao and Wu

(2006b), with the inclusion of the roughness effect through a correction of the boundary conditions. However, the correction works only for small z_0; therefore in actual computations of deposition onto rough surfaces one has to resort to semiempirical models.

A number of experiments on aerosol deposition in laboratory facilities (test chambers) have been conducted recently which confirm the results of the above theoretical researches. Thus, Lai and Nazaroff (2005) studied the deposition of 0.9–9 μm particles onto vertical walls of roughness z_0 ranging from 10 to 250 μm. Hussein et al. (2009) studied the deposition of 0.05–10 μm particles onto smooth walls. In either case friction velocity u^* was slow, from 1 to 12 cm/s. The results agree fairly well with the predictions of Lai and Nazaroff (2000), and Zhao and Wu (2006a, 2006b).

In summary, the derivation of working formulas for aerosol dry deposition over a wide range of external conditions inevitably requires the combination of theoretical and semiempirical approaches as well as a procedure for making the model components consistent with each other. An attempt to solve this problem is presented here, based on the classic papers by Sehmel (1973), Sehmel and Hodgson (1978), Slinn (1978) and the recent theoretical models by Lai and Nazaroff (2000), and Zhao and Wu (2006a, 2006b).

2. Analytical expressions for velocities of deposition onto smooth surfaces

2.1. Brief description of the model of Zhao and Wu (2006a)

To begin, let us enumerate the principal equations of Zhao and Wu (2006a) and their most important assumptions. In what follows we will use the notation of Zhao and Wu (2006a), only replacing v by u for velocities. In the model, the particle flux j onto the boundary is given by

$$j = -(\varepsilon_p + D)\frac{\partial C}{\partial y} - iu_s C + V_t C, \tag{1}$$

where C is the particle concentration, y is a coordinate normal to the surface, $\varepsilon_p$and D are the coefficients of turbulent and Brownian particle diffusion, respectively; i denotes the surface type (0 for vertical, 1 for horizontal (floor), −1 for horizontal (ceiling)), u_s is the sedimentation velocity of particles, V_t is the turbophoresis velocity, which, after appropriate simplifications, can be represented in the form given by Guha (1997)

$$V_t = -\tau_p \frac{d\overline{u'^2_{py}}}{dy}, \tag{2}$$

where τ_p is the particle relaxation (deceleration) time and $\overline{u'^2_{py}}$ is the mean square fluctuation velocity of a particle in direction y. Important assumptions used in the model to describe the inertial motion of particles in turbulent pulsations are the relations between the characteristics of turbulent air pulsations and fluctuating motion of the particles:

$$\overline{u'^2_{py}} = \overline{u'^2_y}\left(1 + \frac{\tau_p}{\tau_L}\right)^{-1}, \quad \frac{\varepsilon_p}{v_t} = \left(1 + \frac{\tau_p}{\tau_L}\right)^{-1}, \tag{3}$$

where τ_L is the Lagrangian timescale of turbulence, v_t is turbulent viscosity. Denoting the concentration far from the boundary layer by C_∞, we introduce a deposition velocity

$$u_d = \frac{j}{C_\infty}, \tag{4}$$

and further dimensionless quantities which will be superscripted by $^+$:

$$C^+ = \frac{C}{C_\infty}, \quad y^+ = \frac{yu^*}{v}, \quad u_d^+ = \frac{u_d}{u^*} \quad \overline{u'^2_{py}}^+ = \frac{\overline{u'^2_{py}}}{u^{*2}},$$

$$\tau^+ = \frac{\tau_p u^{*2}}{v}, \quad \overline{u'^2_y}^+ = \frac{\overline{u'^2_y}}{u^{*2}}, \quad Sc = \frac{v}{D} \quad v_t^+ = \frac{v_t}{v},$$

where v is the molecular viscosity of air, Sc the Schmidt number, and u^* the friction velocity. The dimensional variables make the solution more universal and facilitate the analysis of the results.

In dimensionless variables, Eq. (1) with account for definition (4) becomes

$$u_d^+ = \frac{dC^+}{dy^+}\left[\left(\frac{\tau_L}{\tau_L + \tau_p}\right)v_t^+ + Sc^{-1}\right] + iu_s^+ C^+ + \tau^+ C^+ \frac{d\left[\overline{u'^2_y}^+\left(\frac{\tau_L}{\tau_L + \tau_p}\right)\right]}{dy^+}. \tag{5}$$

Under quasi-stationary conditions flux j and deposition velocity u_d^+ can be considered as constant. Thus (5) becomes a differential equation for the determination of concentrations C^+. Since the boundary conditions are posed on the two ends of the range:

$C^+ = 0$ for $y^+ = 0$ and $C^+ = 1$ for $y^+ = \infty$, to meet the second boundary condition, a self-consistent value of deposition velocity u_d^+ should be taken, which is just the solution to the problem. In reality the boundary conditions are posed by Zhao and Wu (2006a) with $y^+ = r^+$ (here $r^+ = ru^*/v$ is dimensionless particle radius) and with $y^+ = 30$ (this is the actual boundary layer thickness):

$$C^+ = 0 \;\text{ with } y^+ = r^+ \quad \text{and} \quad C^+ = 1 \;\text{ with } y^+ = 30. \tag{6}$$

Lagrangian timescale τ_L and air velocity fluctuations are parameterized in the boundary layer as follows:

$$\tau_L = \frac{v_t}{\overline{u_y'^2}}; \quad \overline{u_y'^2}^+ = \left(\frac{0.005y^{+2}}{1 + 0.002923y^{+2.128}}\right)^2. \tag{7}$$

To determine all quantities appearing in Eq. (5), we give the parametric dependences for the turbulent viscosity in the boundary layer:

$$\begin{aligned} v_t^+ &= 7.669 \cdot 10^{-4}(y^+)^3 && \text{for } 0 \leqslant y^+ \leqslant 4.3, \\ v_t^+ &= 10^{-3}(y^+)^{2.8214} && \text{for } 4.3 \leqslant y^+ \leqslant 12.5, \\ v_t^+ &= 1.07 \cdot 10^{-2}(y^+)^{1.8895} && \text{for } 12.5 \leqslant y^+ \leqslant 30. \end{aligned} \tag{8}$$

2.2. Analysis of the solution and derivation of approximating formulas

We now proceed to develop the general solution to Eq. (5) assuming a constant deposition velocity u_d^+ (hereinafter y will be used without superscript +, the dependence on τ^+or particle diameter d is implied everywhere):

$$C^+(y) = \frac{u_d^+}{p(a,y)} \int_a^y \frac{p(a,z)\,dz}{F(z)}; \quad p(a,y) = \exp\left(\int_a^y \frac{G(z)}{F(z)}\,dz\right),$$

$$F(y) = Sc^{-1} + v_t^+(y)\left(\frac{\tau_L}{\tau_L + \tau_p}\right); \quad G(y) = \tau^+ \frac{d}{dy}\left[\overline{u_y'^2}^+\left(\frac{\tau_L}{\tau_L + \tau_p}\right)\right] + iu_s^+, \tag{9}$$

where constants a and u_d^+ must be selected from the conditions at the boundary layer edges. As a result Zhao and Wu (2006a) obtained the following expression for the deposition velocity:

$$u_d^+ = \frac{p(r^+, 30)}{\int_{r^+}^{30} \frac{p(r^+, y)\,dy}{F(y)}} = \frac{1}{\int_{r^+}^{30} \frac{P(y)\,dy}{F(y)}}; \quad P(y) = \exp\left(-\int_y^{30} \frac{G(z)}{F(z)}\,dz\right). \tag{10}$$

Our numerical calculations suggest that the direct integration of differential Eq. (5) underlying the model of Zhao and Wu (2006a, 2006b), or that of its formal solution (10) is computationally time consuming, because of a severe change in the integration step at different areas of the boundary layer. This dramatically impedes the use of (5) or (10) within the numerical 2D, 3D complexes, as the deposition calculation should be referred to at each timestep.

The analytical and numerical study shows that integrand

$$H(y) = \frac{1}{F(y)} \exp\left[-\int_y^{30} \frac{G(z)\,dz}{F(z)}\right]$$

in the denominator of (10) actually has a singularity as $y \to 0$. On the interval $0 \leqslant y \leqslant 30$ corresponding to the entire boundary layer, the major contributions to integral $J(r^+) = (u_d^+)^{-1} = \int_{r^+}^{30} H(y)\,dy$ are made either by the upper or lower limits of integration. In so doing function $H(y)$ has sharp maxima at the respective ends of the interval $0 \leqslant y \leqslant 30$. According to this behavior of $H(y)$ one can expand the complete integral J as the sum of the contributions from the lower (J_1) and upper (J_2) limits:

$$J(r^+) = \int_{r^+}^{30} H(y)\,dy = J_1(r^+) + J_2,$$

and estimate these terms individually.

We first turn our attention to the contribution from lower limit J_1. The integrand singularity is determined by the term $1/F(y)$. In the function $G(y)$ it is convenient to individualize the turbophoresis and sedimentation contributions:

$$H(y) = \frac{1}{F(y)} \exp\left[-\int_y^{30} \frac{G(z)\,dz}{F(z)}\right] \approx \frac{\exp[-K(\tau^+)]}{F(y)} \exp\left[-iu_s^+ \int_y^{30} \frac{dz}{F(z)}\right],$$

where

$$K(\tau^+) = \tau^+ \int_0^{30} \frac{d}{dy}\left[\overline{u_y'^2}^+\left(\frac{\tau_L}{\tau_L + \tau_p}\right)\right] \frac{dy}{F(y)}$$

Hence,

$$J_1(r^+) \approx \exp[-K(\tau^+)]\int_{r^+}^{30}\frac{dy}{F(y)}\exp\left[-iu_s^+\int_y^{30}\frac{dz}{F(z)}\right] = \frac{\exp[-K(\tau^+)]}{iu_s^+}\left\{1-\exp\left[-iu_s^+\int_{r^+}^{30}\frac{dz}{F(z)}\right]\right\},$$

$$J_1(r^+) \approx \exp[-K(\tau^+)]\int_{r^+}^{30}\frac{dy}{F(y)} \quad \text{with } i=0.$$

In these relations $\exp[-K(\tau^+)]$ describes the turbophoresis contribution in the averaged manner.

The calculations show that the following approximation works well in the practically important ranges of Sc and τ^+: $K(\tau^+) = 1.2\tau^+$. Finally, for the contribution from the lower limit we have

$$J_1(r^+,\tau^+,Sc) = \frac{\exp(-1.2\tau^+)}{iu_s^+(\tau^+)}\{1-\exp[-iu_s^+(\tau^+)\cdot I_{L-N}(r^+,Sc)]\}, \quad i\neq 0,$$

$$J_1(r^+,\tau^+,Sc) = \exp(-1.2\tau^+)\cdot I_{L-N}(r^+,Sc), \quad i=0. \tag{11}$$

For the integral

$$I_{L-N}(r^+,Sc) = \int_{r^+}^{30}\frac{dy}{F(y)}$$

the analytical formula has been derived by Lai and Nazaroff (2000), who consider the small particle deposition without inclusion of turbophoresis:

$$I_{L-N}(r^+,Sc) = [3.64(Sc)^{2/3}(a-b)+39],$$

$$a = \frac{1}{2}\ln\left[\frac{(10.92Sc^{-1/3}+4.3)^3}{Sc^{-1}+0.0609}\right]+\sqrt{3}\tan^{-1}\left[\frac{8.6-10.92Sc^{-1/3}}{10.92\cdot\sqrt{3}\cdot Sc^{-1/3}},\right] \tag{12}$$

$$b = \frac{1}{2}\ln\left[\frac{(10.92Sc^{-1/3}+r^+)^3}{Sc^{-1}+7.669\cdot 10^{-4}(r^+)^3}\right]+\sqrt{3}\tan^{-1}\left[\frac{2r^+-10.92Sc^{-1/3}}{10.92\cdot\sqrt{3}\cdot Sc^{-1/3}}.\right]$$

At this point the estimation of the contribution J_1 from the lower limit is fully completed. By its implication the contribution describes the deposition of small particles, for which the major process is the Brownian diffusion and the turbophoresis effect leads to a small correction $\exp[-K(\tau^+)]$. From (12) we can derive a simple estimator for deposition velocities of small particles in the size range of $0.005 \ll d \ll 1\,\mu$m. For the range inequalities $1 \ll Sc \ll (r^+)^{-3}$ are valid allowing a significant simplification of the expression for integral $I_{L-N}(r^+,Sc)$:

$$(a-b) = 2\pi/\sqrt{3} = 3.628; \quad I_{L-N} \approx 13.204\cdot Sc^{2/3}.$$

On this basis the fine aerosol deposition velocity can be fitted by $u_d \approx 0.0757\cdot u^* Sc^{-2/3}$. Actually this expression works in size range $0.005\,\mu\text{m} \ll d \ll 1\,\mu\text{m}$ for vertical walls and in range $0.005\,\mu\text{m} \ll d \ll 0.5\,\mu\text{m}$ for horizontal ones. Also note that the analytical estimator of integral J_1 allows reconciliation of the models of Lai and Nazaroff (2000) and Zhao and Wu (2006a).

To estimate the contribution J_2 from the upper limit, we make the following, approximate substitution which is valid for function H having a maximum on upper boundary $y = 30$:

$$H(y) = \frac{1}{F(y)}\exp\left[-\int_y^{30}\frac{G(z)\,dz}{F(z)}\right] \approx \frac{1}{F(30)}\exp\left[-\frac{G(30)}{F(30)}\int_y^{30}dz\right].$$

Hence,

$$J_2 \approx \int_0^{30}\frac{dy}{F(30)}\exp\left[-\frac{G(30)}{F(30)}(30-y)\right] = \frac{1-\exp[-30\cdot G(30)/F(30)]}{G(30)}.$$

Using the boundary layer parameterization, we derive the following formula for functions G and F at the upper limit for contribution J_2:

$$J_2(\tau^+,Sc) = \frac{1-\exp\left\{-\gamma(\tau^+,Sc)\left[1+\dfrac{iu_s^+(\tau^+)}{p(\tau^+)}\right]\right\}}{[p(\tau^+)+iu_s^+(\tau^+)]}. \tag{13}$$

Here

$$\gamma(\tau^+, Sc) = \frac{0.4611 \cdot Sc \cdot \tau^+ \cdot (1 + 0.3859 \cdot \tau^+)}{(1 + 0.1193 \cdot \tau^+) \cdot (1 + 0.1193 \cdot \tau^+ + 6.613 \cdot Sc)},$$

$$p(\tau^+) = \frac{\tau^+ \cdot (1 + 0.3859 \cdot \tau^+)}{65.06 \cdot (1 + 0.1193 \cdot \tau^+)^2}. \tag{14}$$

Physically, Eq. (13) provides an estimator for the turbophoresis contribution.

Thus, the final formula for the dimensionless velocity of deposition onto a smooth surface, based on the model of Zhao and Wu (2006a) and the analysis of singularities of the general solution (10), is given by

$$u_d^+ = \frac{1}{J_1(r^+, \tau^+, Sc) + J_2(\tau^+, Sc)},$$

where $J_1(r^+, \tau^+, Sc)$ is determined from (11), (12) and $J_2(\tau^+, Sc)$ from (13), (14). In the dimensional form

$$u_d = \frac{u^*}{J_1(r^+, \tau^+, Sc) + J_2(\tau^+, Sc)}. \tag{15}$$

2.3. Approximation accuracy check

We now turn our attention to the physical meaning of approximation (15) derived above. Calculations in range $d = 10 - 100\,\mu m$ show an abrupt change in the behavior of integrand $H(y)$: first the major contribution to the deposition is made by the boundary layer $y \approx 0$ adjacent to the wall and then by its external boundary $y \approx 30$. It is remarkable that the regimes change at $\tau^+ \approx 1$ and this is a very important criterion for the deposition regime change. For completeness, let us consider the case of the deposition onto a vertical wall ($i = 0$). For $\tau^+ \ll 1$ the leading deposition mechanism is the Brownian diffusion, here the turbophoresis can be neglected and (15) transfers to formula of work (Lai & Nazaroff, 2000):

$$u_d^+ \approx [J_1(r^+, \tau^+, Sc)]^{-1} = [I_{L-N}(r^+, Sc)]^{-1},$$

For large particles with $\tau^+ \gg 1$ the leading deposition mechanism is turbophoresis and the following explicit formula for its contribution that has been derived by us:

$$u_d^+ \approx [J_2(\tau^+, Sc)]^{-1} = \frac{p(\tau^+)}{1 - \exp[-\alpha(\tau^+, Sc)]}. \tag{16}$$

In the intermediate range $1 < \tau^+ < 100$ the contributions J_1 and J_2 can be comparable, and approximation (15) can be of a reduced accuracy for these values of d.

First and foremost we must check the accuracy of our approximation (15), which is designed to replace the computation-intensive solution (10). The calculations were performed with the fixed values of particle density $\rho_p = 1500\,kg\,m^{-3}$ and friction velocity $u^* = 0.341$ m/s; air parameters were taken at standard conditions of $T = 290$ K and $\rho = 1.23\,kg\,m^{-3}$. These conditions correspond to those of the experiments with uranine particles by Sehmel (1973). Deposition velocities in range $d = 10^{-2}$–$10^2\,\mu m$ were then determined by formula (15) and the results were compared to the numerical calculation of integral (10) for a number of values of d.

2.3.1. Deposition onto vertical walls ($i = 0$)

The results are presented in Fig. 1. The calculations by approximation (15) are shown as a solid line, the numerical calculations of integral (10) with markers (circles). The deposition velocity $u_d = u_d^+ \cdot u^*$ is presented in the figure in dimensional units of m/s. The agreement is obviously very good.

2.3.2. Deposition onto a horizontal underlying surface (floor, $i = 1$)

These results are presented in Fig. 2. There is a good agreement for all particle sizes excluding the range d=6–15 μm($1 < \tau^+ < 10$). At $d = 10\,\mu m$ the difference amounts to roughly a factor of two. The reasons were discussed above. It is impossible to find a more suitable approximation to reduce this difference, where it is smaller than the experimental scatter (see Section 3.1). Also note that the range $d = 6$–15 μm is very narrow. Generally, approximation (15) overestimates the exact values and thus serves as a conservative estimator.

It should be noted that the deposition velocity in Fig. 2 is always faster than that in Fig. 1 as it must physically. For example, for a 20-μm-diameter particle the calculation with (15) yields deposition velocities 9.02 and 7.42 cm/s, respectively. The difference between them is approximately equal to the sedimentation velocity.

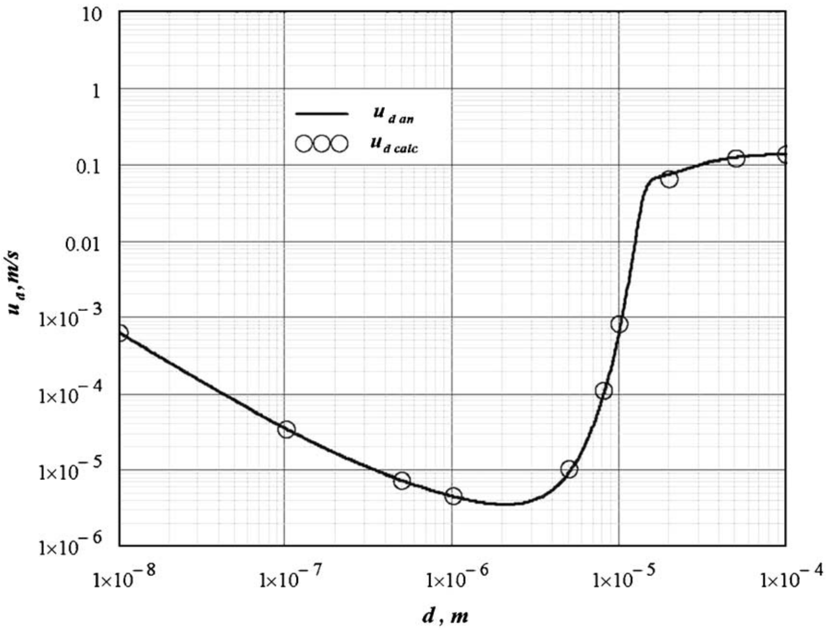

Fig. 1. Deposition onto smooth vertical walls ($i = 0$). $u_{d\,an}$ evaluated with analytic approximation formula (15) against numerical computation of integral (10) $u_{d\,calc}$.

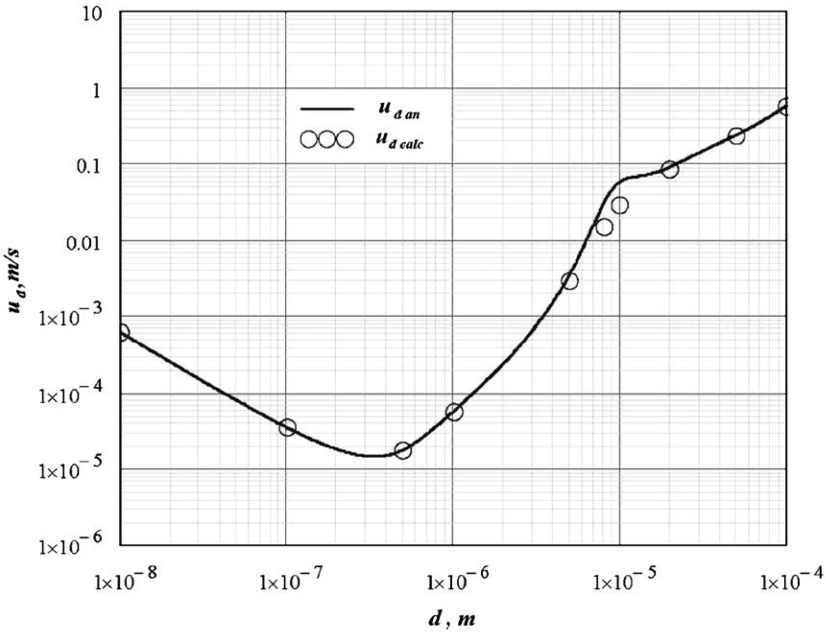

Fig. 2. Deposition onto smooth horizontal surface ($i = 1$). $u_{d\,an}$ evaluated with analytic approximation formula (15) against numerical computation of integral (10) $u_{d\,calc}$.

2.3.3. Deposition onto the ceiling ($i = -1$)

The calculation results are presented in Fig. 3. Either formula results in a crash for particle diameters $d > 5\,\mu\text{m}(\tau^+ > 1)$ in the computations of the velocity of deposition onto ceiling. A reason for this is the divergence of the integral in the expression for

$$P(y) = \exp\left(-\int_y^{30} \frac{G(z)}{F(z)}\,dz\right).$$

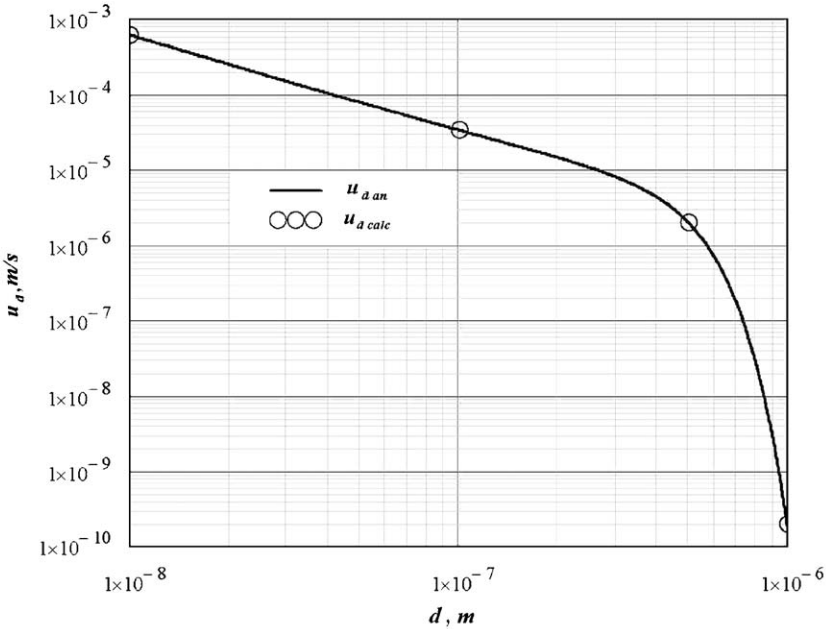

Fig. 3. Deposition onto smooth ceiling ($i = -1$). $u_{d\,an}$ evaluated with analytic approximation formula (15) against numerical computation of integral (10) $u_{d\,calc}$.

From Fig. 3 it is seen, however, that for particles of a diameter larger than 1 μm the deposition velocity is negligible, therefore it can be assumed zero for $\tau^+ > 1$ in practical computations.

The range of application of the above-derived formulas is restricted to a roughness z_0 smaller than the thickness of the first boundary layer zone (in dimensionless units this is $y^+ = 4.3$), hence $z_0 \leqslant 4.3\nu/u^*$. For standard air conditions and friction velocity $u^* \approx 0.6$ m/s these are roughnesses $z_0 \approx 100$ μm. For the calculations with small roughness (for example, in ventilation ducts, in special experiments, on terrain with a smooth underlying surface, viz. snow, water) the above-described models are recommended for use. It should be emphasized that in this case we are dealing with geometric roughness due to surface roughness height. Besides, they are important to make the empirical models consistent with the behavior recommended according to the physical meaning of the deposition processes. For example, in the range of small particle sizes the Brownian diffusion should behave, for which a good approximation is term $0.0757 \cdot u^* Sc^{-2/3}$.

The application to actual terrain conditions with crop covers, bushes and buildings, where $z_0 = 10^{-2}$–1 m, requires a very different class of models, mainly those of empirical nature, which will be dealt with below. In this case the meaning of roughness itself changes: this is the quantity characterizing the logarithmic profile of the flow velocity.

3. Sehmel's semiempirical model for deposition onto very rough surfaces

3.1. Deposition onto a horizontal surface

In this section we will rely on the semiempirical model for the velocity of dry deposition onto a horizontal underlying surface (Kharchenko, 1997; Sehmel, 1973, 1980; Sehmel & Hodgson, 1978), which is typically referred to as Sehmel's model, and experimental data of the paper by Slinn (1978).

The experiments show that the vertical pollutant flux j near the underlying surface is proportional to its surface concentration $C(z)$. Dry deposition velocity $\alpha(z) = j/C(z)$ is typically determined from the measured pollutant concentrations and flux at some height z_{exp} of about 0.1–1 m above the underlying surface.

If we assume that a function for the dry deposition at a height z_{exp} above the surface has been derived on the basis of the experimental data, then it is easy to construct a model predicting the deposition velocity at any surface layer height $z > z_{\mathrm{exp}}$. We represent the deposition velocity α_z at a height z above the surface as

$$\alpha_z = \frac{j}{C(z)} = \frac{u_s}{1 - \exp\left(\frac{u_s}{u^*} Int\right)}.$$

As in Sehmel and Hodgson (1978), the following notation is introduced:

$$Int = \int_z^0 \frac{u^*\,dz}{K_3 + D} = Int_{\mathrm{exp}} + \int_z^{z\,\mathrm{exp}} \frac{u^*\,dz}{K_3 + D} = Int_{\mathrm{exp}} + Int_z,$$

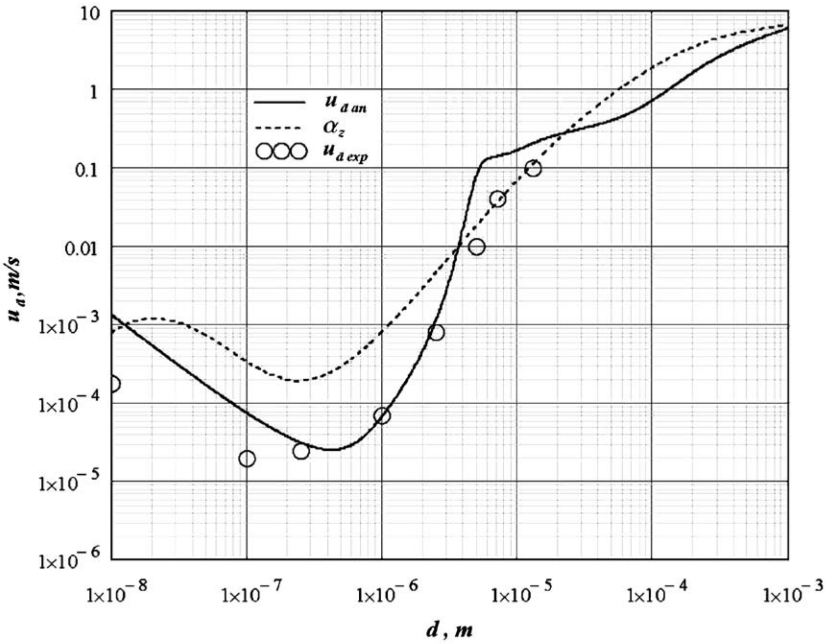

Fig. 4. Experimental velocities $u_{d\,exp}$ of dry deposition onto horizontal surface which are presented by Sehmel (1973) against $u_{d\,an}$ and α_z calculated by approximation formulas (15) and (18) for $z = 0.01$ m, $u^* = 0.726$ m/s, $z_0 = 4 \times 10^{-5}$ m.

where z_{exp} is the height, at which the dry deposition velocity is measured. A so-called drag integral *Int* is divided into two components: Int_{exp} is expressed in terms of the experimental dry deposition velocities

$$Int_{\mathrm{exp}} = \frac{u^*}{u_s} \ln\left(1 - \frac{u_s}{\alpha_{\mathrm{exp}}}\right),$$

while the second integral, Int_z, is taken analytically for any category of atmospheric stability (Kharchenko, 1997):

$$Int_z = \begin{cases} \frac{-1}{k} \ln \frac{z}{z_{\mathrm{exp}}}, |L| = \infty; -\frac{1}{k}\left(\ln \frac{z}{z_{\mathrm{exp}}} + 6\frac{z - z_{\mathrm{exp}}}{L}\right), & L > 0, \\ -\frac{1}{k} \ln \frac{\left(\sqrt{1-\frac{9}{L}z}-1\right)\left(\sqrt{1-\frac{9}{L}z_{\mathrm{exp}}}+1\right)}{\left(\sqrt{1-\frac{9}{L}z}+1\right)\left(\sqrt{1-\frac{9}{L}z_{\mathrm{exp}}}-1\right)}, & L < 0. \end{cases} \tag{17}$$

In (17) L is the Monin–Obukhov scale.

Sehmel and Hodgson (1978) proposed an interpolation expression for the determination of Int_{exp} using the experimental deposition velocities at height $z_{\mathrm{exp}} = 0.01$ m. It turns out, however, that the approximation does not describe the experimental and graphic data presented by Sehmel (1973), Sehmel and Hodgson (1978), Slinn (1978). Apparently, the associated equations are presented by Sehmel and Hodgson (1978) with misprints. Using the experimental material presented by the above authors (mainly in the graphical form), Kharchenko (1997) obtained the following interpolating expression for the dry deposition velocity which is valid for roughness $z_0 \leqslant 10$ cm:

$$\begin{aligned} \ln(-Int_{\mathrm{exp}}) = & -367.8 + 16.4 \ln\left(\frac{\nu}{D}\right) - 0.73 \ln(100d)\ln(10^4 D) - 0.5[\ln(100d)]^2 \\ & + 0.13 \ln\left(\frac{0.03}{z_0}\right) + 0.25 \ln\left(\frac{0.2}{u_*}\right)\left[1 - 0.2 \ln\left(\frac{0.03}{z_0}\right)\right] \\ & - 0.03 \ln \tau_+ \ln\left(\frac{0.03}{z_0}\right) - 32.7 \ln(100d), \end{aligned}$$

$$\alpha_z = \frac{u_s}{1 - \exp\left[\frac{u_s}{u^*}(Int_{\mathrm{exp}} + Int_z)\right]}. \tag{18}$$

In (18) τ_+ is dimensionless particle relaxation time; all the quantities are presented in SI units. Let us validate approximation (18) and verify its accuracy.

For illustration we present the results of the calculations for the deposition velocity of particles of density $\rho_p = 1500\,\mathrm{kg\,m^{-3}}$ at 0.01 m height. The calculations were conducted for the following conditions: standard atmospheric pressure, air temperature

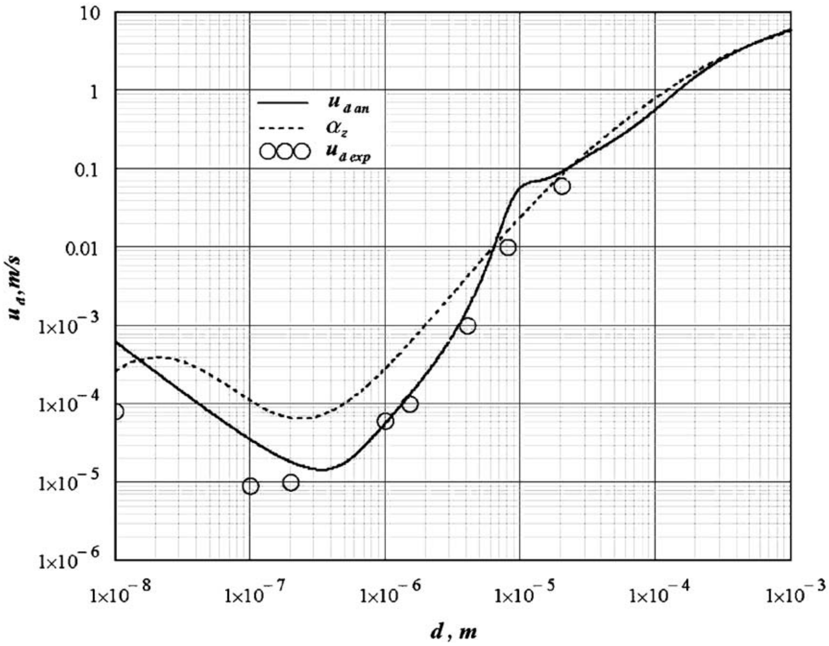

Fig. 5. Experimental velocities $u_{d\,exp}$ of dry deposition onto horizontal surface which are presented by Sehmel (1973) against $u_{d\,an}$ and α_z calculated by approximation formulas (15) and (18) for $z = 0.01$ m, $u^* = 0.341$ m/s, $z_0 = 4 \times 10^{-5}$ m.

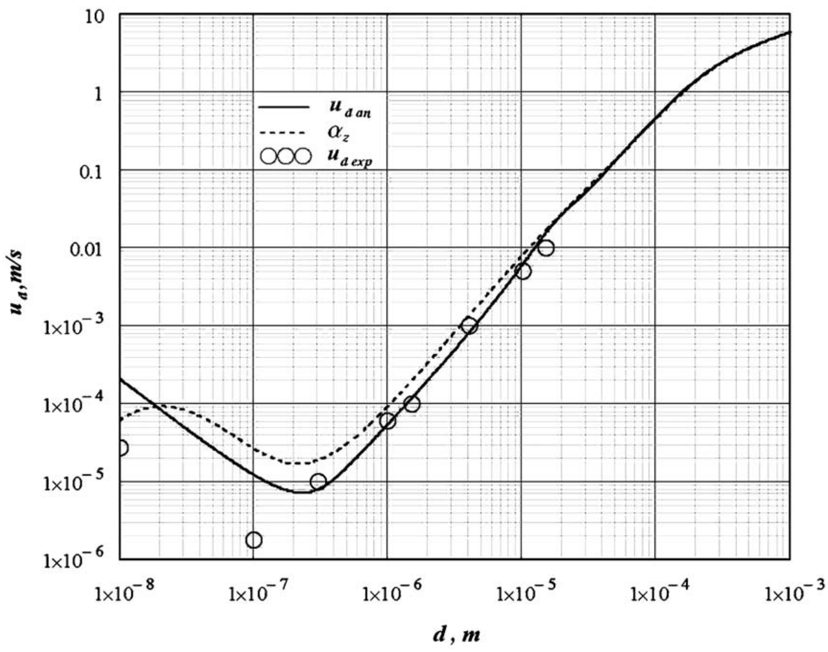

Fig. 6. Experimental velocities $u_{d\,exp}$ of dry deposition onto horizontal surface which are presented by Sehmel (1973) against $u_{d\,an}$ and α_z calculated by approximation formulas (15) and (18) for $z = 0.01$ m, $u^* = 0.114$ m/s, $z_0 = 4 \times 10^{-5}$ m.

290 K. In these conditions, air density is $\rho = 1.22\,\mathrm{kg\,m^{-3}}$, dynamic viscosity is $\mu = 1.8 \cdot 10^{-5}\,\mathrm{N\,s\,m^{-2}}$. Figs. 4–6 compare the calculations to the results of Sehmel (1973) for a small roughness parameter of $z_0 = 40\,\mu$m.

From Figs. 4–6 it is seen that for this roughness parameter the deposition velocities are described well by formula (15) for the smooth surface (solid line). At $d = 0.01$ and 0.1 μm the data of Sehmel (1973) should be hardly regarded as representative, since the measured deposition velocity is smaller than the physical limit for Brownian diffusion, which is described by approximation $0.0757 \cdot u^* Sc^{-2/3}$. Also note that approximation (18) gives a non-physical bend in the vicinity of point $d = 0.01\,\mu$m, but particles of sizes $d < 0.01\,\mu$m are not considered here.

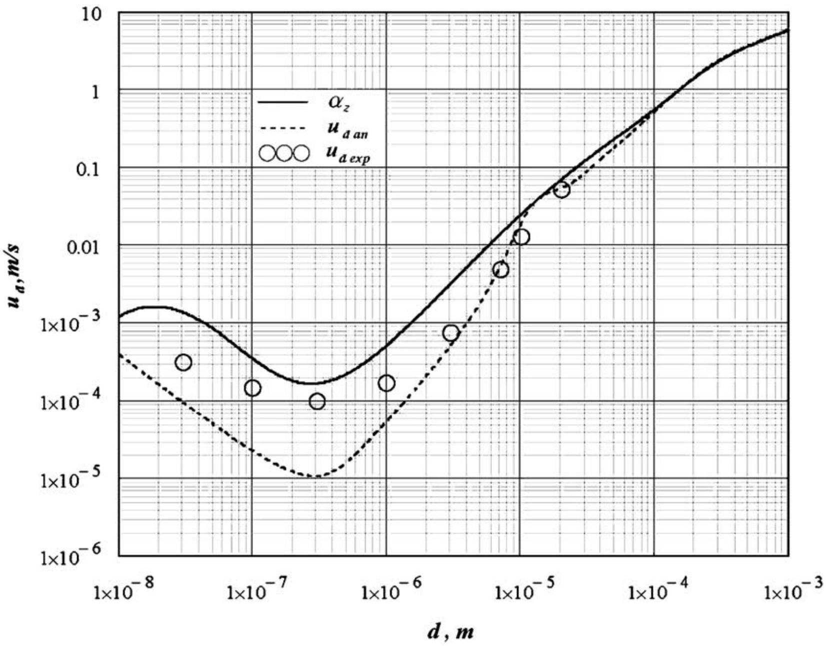

Fig. 7. Experimental velocities $u_{d\,exp}$ of dry deposition onto rough horizontal surface which are presented by Slinn (1978) against $u_{d\,an}$ and α_z calculated by approximation formulas (15) and (18) for $u^* = 0.22$ m/s, $z_0 = 4.7 \times 10^{-3}$ m.

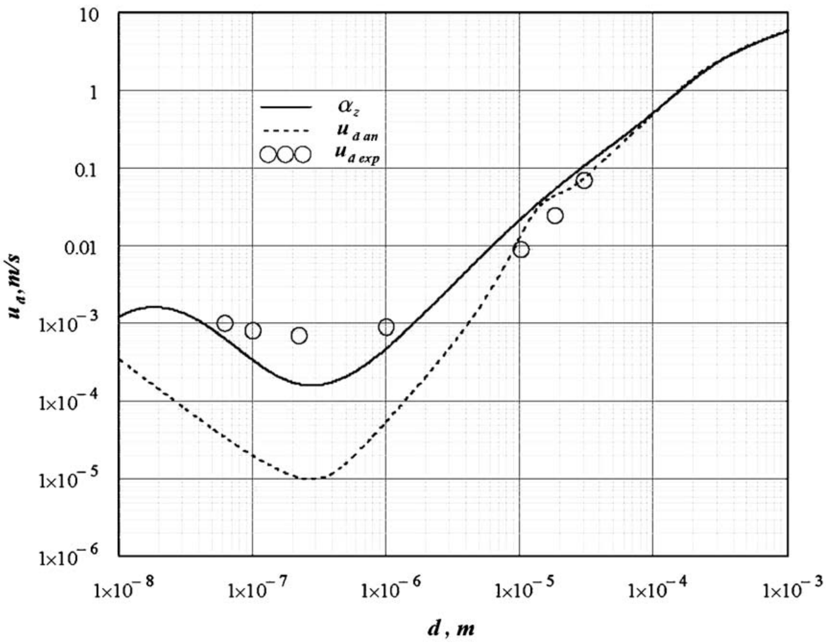

Fig. 8. Experimental velocities $u_{d\,exp}$ of dry deposition onto rough horizontal surface which are presented by Slinn (1978) against $u_{d\,an}$ and $\alpha_z$calculated by approximation formulas (15) and (18) for $u^* = 0.19$ m/s, $z_0 = 7 \times 10^{-3}$ m.

Figs. 7 and 8 compare our calculations to the experimental data by Slinn (1978) for large roughness: $z_0 = 0.47$ and 0.7 mm. For these roughness parameters formula (18) is seen to work better, while from the combination of the results presented in Figs. 4–8 a mutual agreement between theoretical (15) and semiempirical (18) approaches can be observed.

It should be noted that there is a significant scatter in the experimental data presented by Slinn (1978). For example, the experiments plotted in Figs. 7 and 8 were conducted in essentially the same conditions, while deposition velocities differ by about an order of magnitude in the size range $d = 0.1–1$ μm.

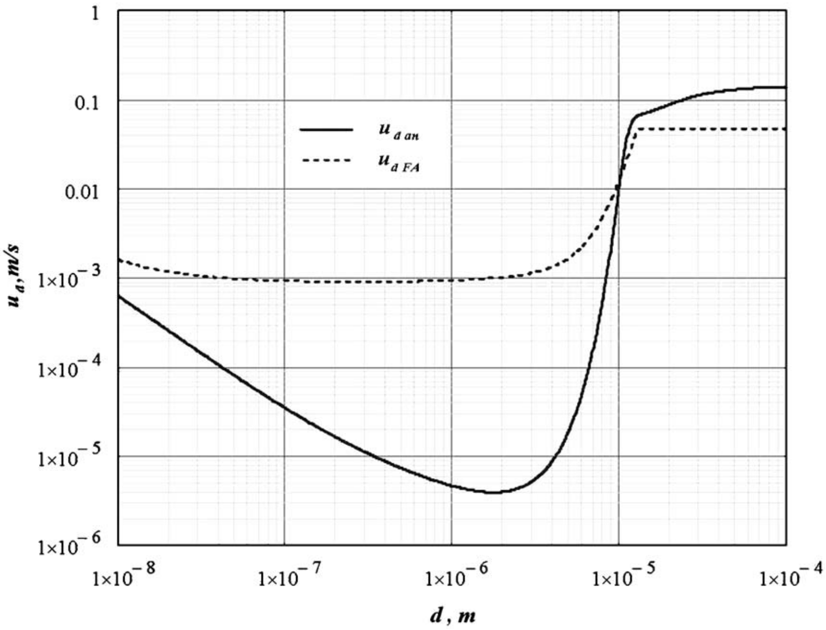

Fig. 9. Calculated velocities of deposition onto vertical walls. $u_{d\,an}$: calculation by (15); $u_{d\,FA}$: calculation by (19) for $u^* = 0.341$ m/s and roughness $z_0 = 4 \times 10^{-5}$ m.

On the whole, the comparison of dry deposition velocities calculated by (17) and (18) with the data of Sehmel and Hodgson (1978) shows no overestimations larger than by an order of magnitude, which corresponds to the scatter in the experimental data. Model (17) and (18) can therefore be recommended to calculate dry deposition velocities for a roughness parameter $z_0 \geqslant 4.3\nu/u^*$.

3.2. Models of deposition onto vertical walls

For smooth vertical walls, the theoretical model presented in Section 2 provides an exhaustive answer in that it accounts completely for important physical processes and provides computationally efficient formulas. As shown in Section 2.3, formula (15) with explicit expressions (11) and (12) for J_1 and J_2 gives an essentially valid answer with $i = 0$. Note that the formula for the deposition onto vertical walls is easy to derive by passage to the limit $u_s \to 0$ from the formulas for the deposition onto a horizontal surface.

Experimental data for the deposition velocity (Davies, 1966; Fan & Ahmadi, 1993; Johansen, 1991; Liu & Agarwal, 1974; Sippola & Nazaroff, 2002; Wood, 1981a) are limited, mainly, to measurements in small-diameter pipes, paths of physical facilities or ventilation ducts. As a rule, these measurements are taken only for a small roughness parameter, in the range of hundreds of micrometers. However, calculations of pollutant transport in an urban environment require deposition velocities for a roughness scale as large as several centimeters, which are obtained in the wall relief averaging (the presence of window openings, inclusion of geometry of masonry, etc.) within the mesh scale. Since experimental data in this area are missing, it will be necessary to use cross-linking with the results for smooth walls, extrapolation of computed data from physical considerations, and making asymptotics in the range of large and small particle sizes.

A most extensively quoted model of deposition onto vertical walls with inclusion of roughness is the experiment based semiempirical model of Fan and Ahmadi (1993), in which the dimensionless deposition velocity u_d^+ is given by

$$F_1 = (1 + \tau^{+2} L_1^+)^{-1}; \quad F_2 = 92.166\tau^{+2} g^+ L_1^+ F_1; \quad F_3 = 0.037[1 - \tau^{+2} L_1^+ (1 + g^+/0.037]^{-1};$$
$$L_1^+ = 3.08/(d^+ S),$$

$$u_d^+ = 0.084 Sc^{-2/3} + \frac{1}{2}\left[\frac{(0.064k^+ + d^+/2) + F_2}{3.42 + F_2}\right]^{F_1} [1 + 8e^{-(\tau^+ - 10)^2/32}] F_3 \quad \text{if} \;\; u_d^+ < 0.14,$$
$$u_d^+ = 0.14 \;\; \text{if} \;\; u_d^+ > 0.14, \quad u_d^+ = 0.14 \;\; \text{if} \;\; u_d^+ < 0, \tag{19}$$

where k^+ is roughness in dimensionless units, S is the ratio of particle and air densities. In this model the velocity of deposition (of large particles) does not exceed 0.14 u^*. For small particle sizes a physically correct asymptotic behavior $u_d^+ \sim Sc^{-2/3}$ is observed.

Figs. 9 and 10 compare the calculations by the model of Section 2.2 for a smooth wall (see (15)) and calculations by (19) for friction velocity $u_* = 0.341$ m/s and roughnesses $z_0 = 40$ and 200 μm. The dashed line corresponds to the calculation by (19) and the solid line to that by (15). The deposition velocities calculated by (19) are seen to be significantly larger than those determined

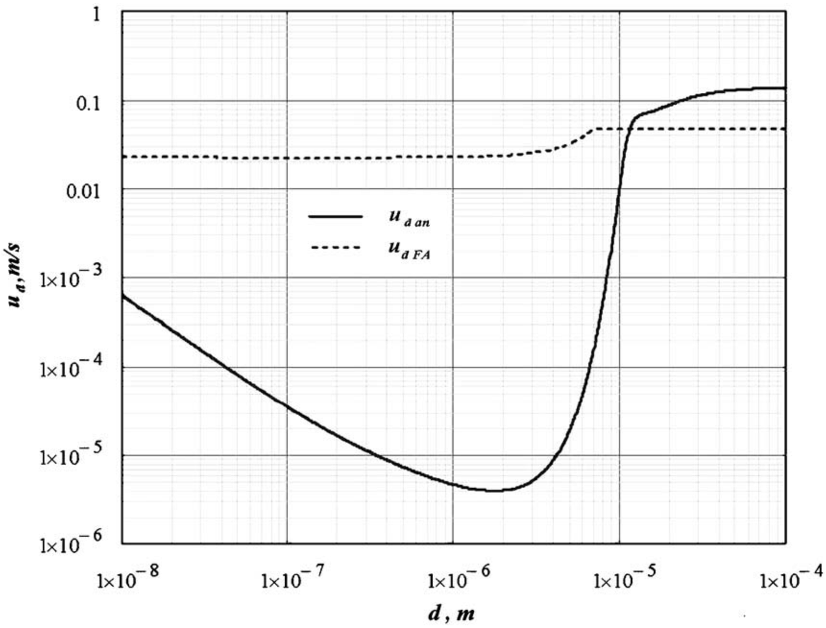

Fig. 10. Calculated velocities of deposition onto rough vertical walls. $u_{d\,an}$: calculation by (15); $u_{d\,FA}$: calculation by (19) for $u^* = 0.341$ m/s and roughness $z_0 = 2 \times 10^{-4}$ m.

by (15) for the smooth wall, even for a small roughness of $z_0 = 40\,\mu$m. Moreover, the velocities determined by (19) for $z_0 = 200\,\mu$m remain essentially unchanged in the entire particle size range $d = 0.01–100\,\mu$m, that is the result of application of this model is insufficiently informative. On the whole, the data determined by model (19) disagrees with the experimental results of Sehmel (1973). For this reason model (19) will not be considered hereafter.

Thus, the need arises to develop a new model applicable for moderate roughnesses of $z_0 \approx 1$ cm. For this purpose we will make use of the theoretical considerations and derivation leading to Sehmel's model for horizontal surfaces. As already mentioned, in the theoretical model analyzed in Section 2.2 the deposition velocities for vertical walls are determined by passage to the limit $u_s \to 0$ from the formulas for deposition onto a horizontal surface. This passage is based on the fact that the boundary layer is described identically in the two cases and the sedimentation effect is included explicitly—using the additional term for function $G(y)$ in (9). Let us make use of the same technique for a modified semiempirical Sehmel model (18), which we have selected as the basic model for calculation of the deposition onto the horizontal surface (note in passing that here there is no need to include atmospheric profiles). Let us choose the constant in (18) so that for large particle sizes the deposition velocity behavior correspond to (15) at $i = 0$ (see Figs. 11 and 12). This leads to the following working formula for vertical surfaces:

$$\ln(-Int_{\mathrm{exp}}) = -365.5 + 16.4 \ln\left(\frac{\nu}{D}\right) - 0.73 \ln(100d) \ln(10^4 D) - 0.5[\ln(100d)]^2 + 0.13 \ln\left(\frac{0.03}{z_0}\right) + 0.25 \ln\left(\frac{0.2}{u*}\right)\left[1 - 0.2 \ln\left(\frac{0.03}{z_0}\right)\right] - 0.03 \ln \tau_+ \ln\left(\frac{0.03}{z_0}\right) - 32.7 \ln(100d),$$

$$\alpha = \frac{u^*}{Int_{\mathrm{exp}}}. \tag{20}$$

Figs. 11 and 12 compare the calculations by (20) to those by (15) at $i = 0$ and to the experimental data of Sehmel (1973) that were measured for a small roughness of $z_0 = 40\,\mu$m. It should be noted once more that the data of Sehmel (1973) for $d < 1\,\mu$m are hardly representative, as they are below the physical limit for Brownian diffusion. Apparently, Sehmel (1973) plotted them as a rough extrapolation.

Both (15) and (20) yield a qualitative agreement with the data of Sehmel (1973), but model (20) for rough vertical surfaces works better. This is not a very consistent result, as roughness parameter $z_0 = 40\,\mu$m satisfies condition $z_0 < 4.3\nu/u^*$. On the whole, however, the agreement is fairly good and approximation (20) can be recommended for use in calculations of the deposition onto vertical walls.

This paper does not touch on deposition of particles on vegetative canopies. This is a complex, multifactor problem requiring inclusion of a real geometry of the absorbing surface and reproduction of a complex pattern of flows. Certain success in solution of this problem is demonstrated by Petroff, Mailliat, Amielh, and Anselmet (2008a, 2008b), who reviewed and analyzed a great body of models and experimental data. The results of the analysis have been implemented in a new model, whose application is exemplified by Petroff, Zhang, Pryor, and Belot (2009).

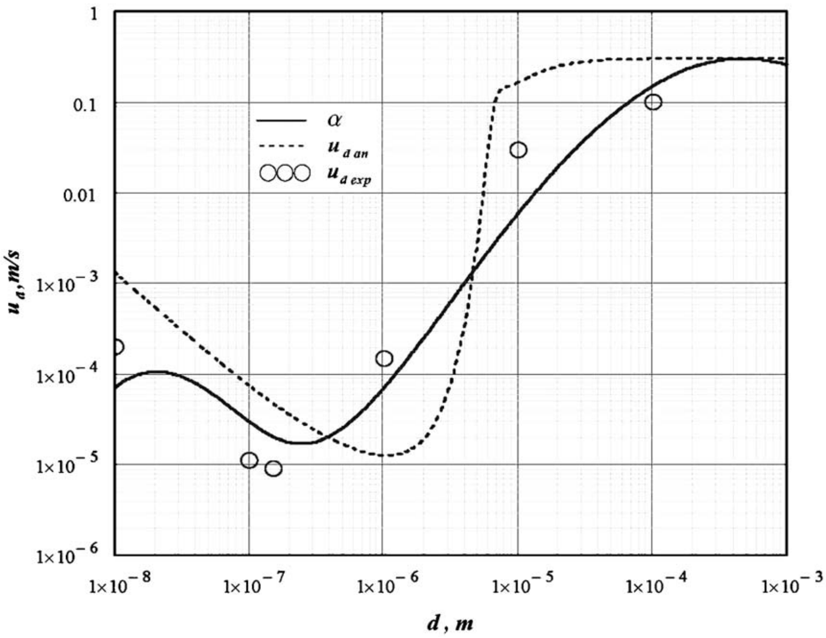

Fig. 11. Experimental velocities $u_{d\,exp}$ of dry deposition onto vertical walls which are presented by Sehmel (1973) against $u_{d\,an}$ and α calculated by approximation formulas (15) and (20) for $u^* = 0.726$ m/s, $z_0 = 4 \times 10^{-5}$ m.

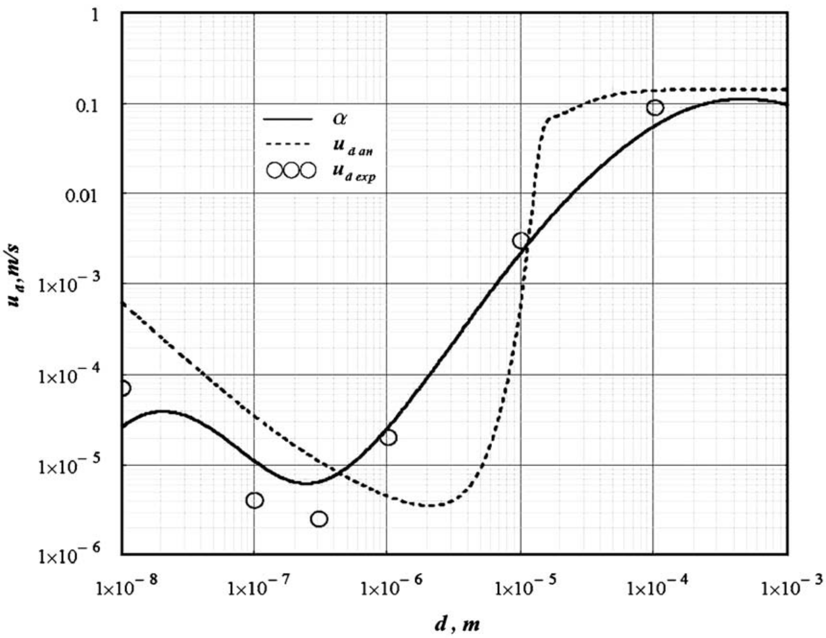

Fig. 12. Experimental velocities $u_{d\,exp}$ of dry deposition onto vertical walls which are presented by Sehmel (1973) against $u_{d\,an}$ and α calculated by approximation formulas (15) and (20) for $u^* = 0.341$ m/s, $z_0 = 4 \times 10^{-5}$ m.

4. Summary and conclusions

The 2D and 3D calculations of aerosol deposition require working formulas for the dry deposition velocities applicable to the urban and indoor environments which should meet quite various requirements:

- applicability for deposition onto vertical and horizontal surfaces;
- function over a wide range of particle sizes d and surface roughness parameters z_0;
- simplicity of the formulas enabling real-time computations.

It is for this reason that the derivation of the working formulas for aerosol deposition in a wide range of external conditions inevitably requires a combination of theoretical and semiempirical approaches and procedures for reconciliation of the approaches. An attempt to solve this problem is presented in this paper. The classic papers by Sehmel (1973), Sehmel and Hodgson (1978), Slinn (1978) and theoretic models by Lai and Nazaroff (2000), and Zhao and Wu (2006a, 2006b) are taken as a basis.

The analysis of the features of general solution (10) obtained by Zhao and Wu (2006a) for smooth surfaces allows us to single out contributions of the major processes, derive suitable analytical formulas for integrals, and reconcile the models by Lai and Nazaroff (2000) and Zhao and Wu (2006a). The results of the recent experimental papers by Lai and Nazaroff (2005), and Hussein et al. (2009) on fine aerosol deposition agree fairly well with the predictions by Lai and Nazaroff (2000), Zhao and Wu (2006a, 2006b) and, hence, with our data.

For rough surfaces most reliable remain the experimental data on dry deposition velocity onto horizontal substratum by Sehmel (1973, 1980), Sehmel and Hodgson (1978), and Slinn (1978), . The semiempirical model by Sehmel and Hodgson (1978) and Kharchenko (1997) that has been developed using them allows calculating the deposition onto horizontal surfaces with roughness $z_0 \leqslant 10$ cm. This paper extends the model to the deposition onto vertical walls.

The effort resulted in simple formulas to calculate velocities of deposition onto smooth and rough surfaces that are valid in a wide range of particle sizes $0.01 \leqslant d \leqslant 1000\,\mu$m and surface roughness $z_0 \leqslant 10$ cm.

In outline the procedure is as follows:

1. The velocity of deposition onto a smooth surface (horizontal or vertical) is calculated using working formula (15), where J_1 is determined from (11) and (12) and J_2 from (13) and (14).
2. The velocity of deposition onto a rough surface with parameter $z_0 \geqslant 4.3\nu/u^*$ is calculated by formula (18) for the horizontal surface and by formula (20) for the vertical surface.

The results can be used for 2D and 3D computations of the aerosol deposition onto vertical and horizontal surfaces in the urban and indoor environments as well as for operational evaluation. Emphasize that this paper does not touch on the particle deposition onto vegetative canopies.

References

Chen, F., Yu, S. C. M., & Lai, A. C. K. (2006). Modeling particle distribution and deposition in indoor environments with a new drift–flux model. *Atmospheric Environment*, *40*, 357–367.

Davies, C. N. (1966). Deposition of aerosols from turbulent flow through pipes. *Proceedings of Royal Society A*, *289*, 235–246.

Fan, F., & Ahmadi, G. (1993). A sublayer model for turbulent deposition of particles in vertical ducts with smooth and rough surfaces. *Journal of Aerosol Science*, *24*, 45–64.

Gao, N. P., & Niu, J. L. (2007). Modeling particle dispersion and deposition in indoor environments. *Atmospheric Environment*, *41*, 3862–3876.

Guha, A. (1997). A unified Eulerian theory of turbulent deposition to smooth and rough surfaces. *Journal of Aerosol Science*, *28*, 1517–1537.

Hussein, T., Hruška, A., Dohányosová, P., Džumbová, L., Hemerka, J., Kulmala, M. et al. (2009). Deposition rates on smooth surfaces and coagulation of aerosol particles inside a test chamber. *Atmospheric Environment*, *43*, 905–914.

Johansen, S. T. (1991). The deposition of particles on vertical walls. *International Journal of Multiphase Flow*, *17*, 355–376.

Jonsson, L., Karlsson, E., & Jönsson, P. (2008). Aspects of particulate dry deposition in the urban environment. *Journal of Hazardous Materials*, *153*, 229–243.

Kharchenko, A. I. (1997). Parameterization of dry deposition velocity in the atmospheric surface layer. *Journal of Aerosol Science*, *28*(Suppl. 1), 589–590.

Kosovic, B., Sugiyama, G., Chow, T. K., Hanley, W., Johannesson, G., Larsen, S., et al. (2005). Dynamic data-driven event reconstruction for atmospheric releases. *Abstracts of papers at conference on aerosols and safety—2005* p.46. Obninsk, Russia.

Lai, A. C. K., & Nazaroff, W. W. (2000). Modeling indoor particle deposition from turbulent flow onto smooth surfaces. *Journal of Aerosol Science*, *31*, 463–476.

Lai, A. C. K., & Nazaroff, W. W. (2005). Supermicron particle deposition from turbulent chamber flow onto smooth and rough vertical surfaces. *Atmospheric Environment*, *39*, 4893–4900.

Liu, B. Y. H., & Agarwal, J. K. (1974). Experimental observation of aerosol deposition in turbulent flow. *Journal of Aerosol Science*, *5*, 145–155.

Nho-Kim, E. Y., Michou, M., & Peuch, V. H. (2004). Parameterization of size-dependent particle dry deposition velocities for global modeling. *Atmospheric Environment*, *38*, 1933–1942.

Petroff, A., Mailliat, A., Amielh, M., & Anselmet, F. (2008a). Aerosol dry deposition on vegetative canopies. Part I: Review of present knowledge. *Atmospheric Environment*, *42*, 3625–3653.

Petroff, A., Mailliat, A., Amielh, M., & Anselmet, F. (2008b). Aerosol dry deposition on vegetative canopies. Part II: A new modelling approach and applications. *Atmospheric Environment*, *42*, 3654–3683.

Petroff, A., Zhang, L., Pryor, S. C., & Belot, Y. (2009). An extended dry deposition model for aerosols onto broadleaf canopies. *Journal of Aerosol Science*, *40*, 218–240.

Sehmel, G. A. (1973). Particle eddy diffusivities and deposition for isothermal flow and smooth surfaces. *Journal of Aerosol Science*, *4*, 125–138.

Sehmel, G. A. (1980). Particle and gas dry deposition: A review. *Atmospheric Environment*, *14*, 983–1011.

Sehmel, G. A., & Hodgson, W. J. (1978). A model for predicting dry deposition of particles and gases to environmental surfaces. In: *PNL-SA-6721*. Richland, WA: Battelle, Pacific Northwest Laboratory.

Sippola, M. R., & Nazaroff, W. W. (2002). *Particle deposition from turbulent flow: Review of published research and its applicability to ventilation ducts in commercial buildings. Report LBNL-51432,* Lawrence Berkeley National Laboratory.

Slinn, W. G. N. (1978). Parameterization for resuspension and for wet and dry deposition of particles and gases for use in radiation dose calculations. *Nuclear Safety*, *19*(2), 205–219.

Slinn, W. G. N. (1982). Prediction for particle deposition to vegetative canopies. *Atmospheric Environment*, *16*, 1785–1794.

Valentine, J. R., & Smith P. J. (2005). *Numerical predictions of deposition with a particle cloud tracking technique*. Salt Lake City: Reaction Engineering International. ⟨http://www.reaction-eng.com/downloads/deposit.pdf⟩.

Wood, N. B. (1981a). The mass transfer of particles and acid vapour to cooled surfaces. *Journal of the Institute of Energy*, *76*, 76–93.

Wood, N. B. (1981b). A simple method for the calculation of turbulent deposition to smooth and rough surfaces. *Journal of Aerosol Science*, *12*, 275–290.

Yang, Y., & Shao, Y. (2008). Numerical simulations of flow and pollution dispersion in urban atmospheric boundary layers. *Environmental Modelling and Software*, *23*, 906–921.
Zaichik, L. I., & Alipchenkov, V. M. (2007). *Statistical models of particle motion in turbulent fluid*. Moscow: Fizmatlit Publishers, 312pp. (in Russian).
Zhao, B., & Wu, J. (2006a). Modeling particle deposition from fully developed turbulent flow in ventilation duct. *Atmospheric Environment*, *40*, 457–466.
Zhao, B., & Wu, J. (2006b). Modeling particle deposition onto rough walls in ventilation duct. *Atmospheric Environment*, *40*, 6918–6927.
Zhao, B., & Wu, J. (2007). Particle deposition in indoor environments: Analysis of influencing factors. *Journal of Hazardous Materials*, *147*, 439–448.